Angle and Time of Arrival Statistics for a Far Circular Scattering Model

Akshaya Mittal, R. Bhattacharjee, and B. S. Paul
Department of Electronics and Communication Engineering, IIT Guwahati
Email: {akshaya@iitg.ernet.in, ratnajit@iitg.ernet.in, babusena@iitg.ernet.in}

***Abstract*—To exploit the capacity and performance gains associated with the use of antenna arrays, wireless communication systems require proper understanding of the spatial characteristics of the channel. Scattering models provide both Angle of Arrival (AoA) and Time of Arrival (ToA) statistics of the channel. In this paper, we investigate geometrically based single bounce model that assumes that multipath reflection is caused by scatterers located far from the base station (BS) and mobile station (MS). For this model, analytical expressions for the joint ToA/AoA and the marginal AoA probability density functions (pdf's) are derived. The results presented in this paper are expected to provide better understanding of the effect of far scatterers.**

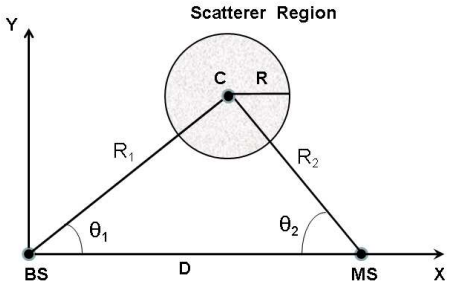

Fig. 1. Scatterer geometry.

I. Introduction

Antenna arrays with optimum combining, combat multipath fading of the desired signal and suppress interfering signals, thereby increasing both the performance and capacity of wireless communication systems. To evaluate the performance of a wireless communication system using antenna arrays as well as to study the spatial properties of the received fading signal, it becomes necessary to have spatial channel models. Spatial channel modeling is performed taking into account the location of scatterers/reflectors that describe the Angle of arrival (AoA) and Time of arrival (ToA) of the multipath components [1], [2]. Geometrically based single bounce model is a widely used radio propagation model, where propagation between transmitting and receiving antennas is assumed to take place via single scattering from an intervening obstacle. The complete behaviour of wireless communication systems may be described by taking the effect of both local scatterer cluster and far scatterer cluster simultaneously [3]–[5]. Local scatterer cluster is located around the mobile station. Various scattering models for the local scatterers have been proposed including circular [6] and gaussian [7] density scatterers. Far scatterers, correspond to high-rise buildings (in urban environments) or mountains (in rural environments), are located far from BS and MS [1]. The use of far scatterer clusters has been recommended both in the European COST259, which developed a generic spatial channel model that is suitable for a wide range of systems, and by the joint "spatial channel modeling" group of 3GPP and 3GPP2, the standardization organizations for third-generation cellular systems [3]–[5]. Here we consider only the effect of far scatterers. This model assumes a uniform distribution for the position of scatterers within a circle which is far from the BS and MS. The joint ToA/AoA pdf and marginal AoA pdf at both the BS and MS are derived for the far scatterer model. Simulation results for marginal AoA and ToA pdf are also provided.

The rest of this paper is organised as follows: Section II presents the model geometry for far scatterers. In Section III and IV, we derive the analytical expressions for the joint ToA/AoA pdf and marginal AoA pdf for the model under consideration respectively. In Section V, the simulation result for marginal ToA pdf has been presented. Section VI concludes the paper.

II. Geometry and Assumptions

Fig. 1 illustrates the distant scatterer channel model. The BS is assumed to be located at the origin and BS and MS are separated by a distance D. It is further assumed that propagation takes place in the horizontal plane containing the tips of the MS and BS antennas.

$$f_{\tau,\theta_b}(\tau,\theta_b) = \begin{cases} \frac{(D^2-\tau^2c^2)(D^2c+\tau^2c^3-2\tau c^2 D\cos(\theta_b))}{4\pi R^2(D\cos(\theta_b)-\tau c)^3}, & \frac{(D^2-\tau^2c^2-2R_1\cos(\theta_b-\theta_1)(D\cos(\theta_b)-\tau c))^2}{4(D\cos(\theta_b)-\tau c)^2} \le R^2 - R_1^2\sin^2(\theta_b-\theta_1) \\ 0, & \text{else.} \end{cases} \tag{11}$$

$$f_{\tau,\theta_s}(\tau,\theta_s) = \begin{cases} \frac{(D^2-\tau^2c^2)(D^2c+\tau^2c^3-2\tau c^2 D\cos(\theta_s))}{4\pi R^2(D\cos(\theta_s)-\tau c)^3}, & \frac{(D^2-\tau^2c^2-2R_2\cos(\theta_s-\theta_2)(D\cos(\theta_s)-\tau c))^2}{4(D\cos(\theta_s)-\tau c)^2} \le R^2 - R_2^2\sin^2(\theta_s-\theta_2) \\ 0, & \text{else.} \end{cases} \tag{15}$$

The scatterers are assumed to be far from BS and MS and uniformly distributed within a circle of radius R. The received signal at the antenna undergoes no more than single scattering by scatterers when traveling from transmitter to receiver. The center of the circle is at a distance R_1 from the BS and makes an angle θ_1 with the line joining BS and MS. The distance between MS and center of the circle is R_2 and line joining the center of the circle and MS makes an angle θ_2 with the line joining MS and BS.

$$R_2 = \sqrt{R_1^2 + D^2 - 2R_1 D\cos(\theta_1)}\,. \tag{1}$$

$$\theta_2 = \tan^{-1}\left(\frac{R_1\sin(\theta_1)}{D - R_1\cos(\theta_1)}\right). \tag{2}$$

III. Joint ToA/AoA pdf

To predict the performance of wideband multisensor arrays, informations regarding the signal multipath delay i.e time of arrival (ToA) and angle of arrival (AoA) are needed. A scatterer in a wireless channel contributes a ray with a given delay and along a given direction. So joint ToA/AoA pdf provides ToA and AoA information for a particular scatterer. The Scatterers are assumed to be uniformly distributed within a circle of radius R, then Scatterer density function is given by

$$f_{x,y}(x,y) = \begin{cases} \frac{1}{A}, & x \text{ and } y \in R_A \\ 0, & \text{else.} \end{cases} \tag{3}$$

Area of the scattering region is $A = \pi R^2$. Scatterer density function can also be represented in polar coordinates (r_b, θ_b), shown in Fig. 2 [8].

$$f_{r_b,\theta_b}(r_b,\theta_b) = r_b f_{x,y}(r_b\cos(\theta_b), r_b\sin(\theta_b)). \tag{4}$$

A. Joint ToA/AoA pdf at the Base Station:

The total path propagation delay is given by

$$\tau = \frac{r_b + r_s}{c} = \frac{1}{c}\left(r_b + \sqrt{D^2 + r_b^2 - 2r_b D\cos(\theta_b)}\right). \tag{5}$$

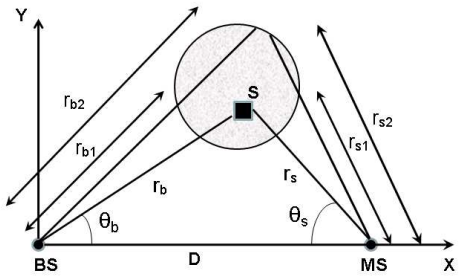

Fig. 2. Polar coordinate representation.

Squaring both the sides of (5) and solving for r_b results in

$$r_b = \frac{D^2 - \tau^2c^2}{2(D\cos(\theta_b) - \tau c)}\,. \tag{6}$$

Interchanging the variables in (4), reduces to

$$f_{\tau,\theta_b}(\tau,\theta_b) = \frac{(D^2-\tau^2c^2)(D^2c+\tau^2c^3-2\tau c^2 D\cos(\theta_b))}{4A(D\cos(\theta_b)-\tau c)^3} \tag{7}$$

Now, we have to find out the range of τ and θ_b for which $f_{\tau,\theta_b}(\tau,\theta_b) \neq 0$. Considering the geometry of scatterers

$$(x - R_1\cos(\theta_1))^2 + (y - R_1\sin(\theta_1))^2 \le R^2 \tag{8}$$

Transforming into polar coordinates gives

$$r_b^2 - 2r_b R_1\cos(\theta_b - \theta_1) + R_1^2 \le R^2 \tag{9}$$

Substituting the expression found for r_b in (6) and then simplifying results in

$$\frac{(D^2 - \tau^2c^2 - 2R_1\cos(\theta_b-\theta_1)(D\cos(\theta_b)-\tau c))^2}{4(D\cos(\theta_b)-\tau c)^2} \le R^2 - R_1^2\sin^2(\theta_b-\theta_1). \tag{10}$$

The Joint ToA/AoA pdf at BS is given by (11), shown at the top of the page.

$$f_{\theta_b}(\theta_b) = \begin{cases} \dfrac{2R_1\cos(\theta_b-\theta_1)\sqrt{R_1^2\cos^2(\theta_b-\theta_1)-R_1^2+R^2}}{\pi R^2}, & \theta_1-\sin^{-1}\left(\dfrac{R}{R_1}\right)\le\theta_b\le\theta_1+\sin^{-1}\left(\dfrac{R}{R_1}\right) \\ 0, & \text{else.} \end{cases} \tag{20}$$

B. Joint ToA/AoA pdf at the Mobile Station:

Due to the symmetry of the geometry, the joint ToA/AoA pdf at MS will have the same form as the joint ToA/AoA pdf at BS. The only difference between the two is the range of τ and θ_b where the pdf is nonzero. The relationship between r_s and τ,

$$r_s = \frac{D^2-\tau^2c^2}{2(D\cos(\theta_s)-\tau c)}. \tag{12}$$

The Joint ToA/AoA pdf at MS is shown in (15) at the top of the previous page, where the range of τ and θ_s for which $f_{\tau,\theta_b}(\tau,\theta_b)\neq 0$ is found by considering the condition on the original scatterer density, namely

$$r_s^2 - 2r_sR_2\cos(\theta_s-\theta_2)+R_2^2\le R^2 \tag{13}$$

Substituting the value of r_s and then simplifying results in

$$\frac{(D^2-\tau^2c^2-2R_2\cos(\theta_s-\theta_2)(D\cos(\theta_s)-\tau c))^2}{4(D\cos(\theta_s)-\tau c)^2} \le R^2 - R2^2\sin^2(\theta_s-\theta_2). \tag{14}$$

Closed form expressions for marginal AoA and ToA pdf could be found by direct integrating the joint ToA/AoA pdf given by (11) and (15), but it is a very difficult approach. However, AoA and ToA pdf may be obtained by performing the integration using numerical methods. Therefore, we consider alternative approach reported in literature [6] to formulate marginal AoA and ToA pdf without involving joint pdf expression.

IV. Marginal AoA pdf

A. AoA pdf at the Base Station:

For a uniform scatterer density, the AoA pdf at BS is given by [8]

$$f_{\theta_b}(\theta_b) = \frac{1}{2A}\left(r_{b2}^2(\theta_b)-r_{b1}^2(\theta_b)\right) \tag{16}$$

The functions $r_{b1}(\theta_b)$ and $r_{b2}(\theta_b)$ are obtained from the polar coordinate representations of the boundary of the scatterer region as shown in Fig. 2.

$$r_b^2 - 2r_bR_1\cos(\theta_b-\theta_1)+R_1^2-R^2=0 \tag{17}$$

Solving quadratic equation (17), we get

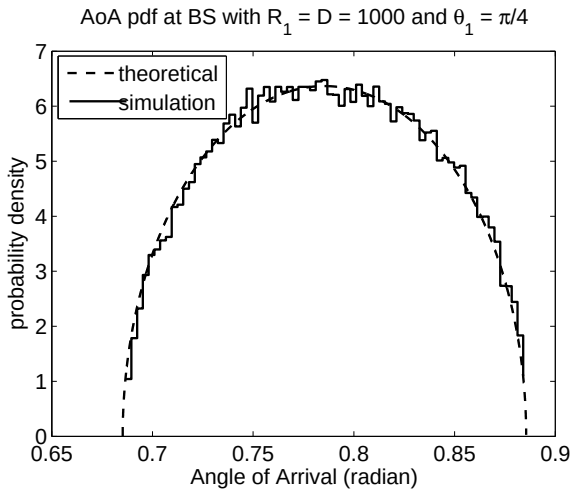

Fig. 3. AoA pdf at BS.

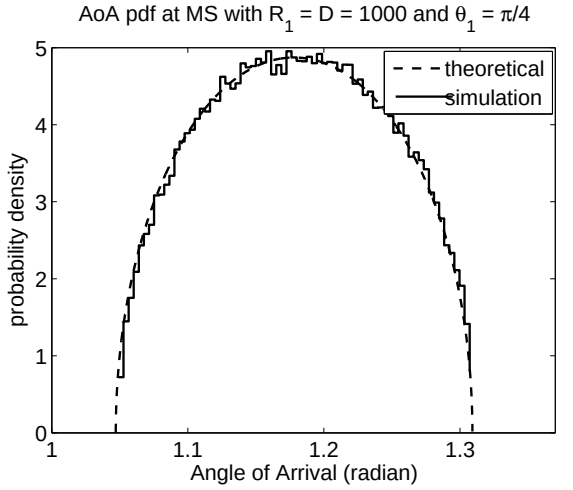

Fig. 4. AoA pdf at MS.

$$r_{b1}(\theta_b) = R_1\cos(\theta_b-\theta_1) - \sqrt{R_1^2\cos^2(\theta_b-\theta_1)-R_1^2+R^2} \tag{18}$$

$$r_{b2}(\theta_b) = R_1\cos(\theta_b-\theta_1) + \sqrt{R_1^2\cos^2(\theta_b-\theta_1)-R_1^2+R^2} \tag{19}$$

Substituting (18) and (19) into (16) with $A=\pi R^2$ and simplifying results in (20), shown at the top of the

$$f_{\theta_s}(\theta_s) = \begin{cases} \dfrac{2R_2\cos(\theta_s-\theta_2)\sqrt{R_2^2\cos^2(\theta_s-\theta_2)-R_2^2+R^2}}{\pi R^2}, & \theta_2-\sin^{-1}\left(\dfrac{R}{R_2}\right) \le \theta_s \le \theta_2+\sin^{-1}\left(\dfrac{R}{R_2}\right) \\ 0, & \text{else.} \end{cases} \tag{24}$$

$$\tau_{\min} = \frac{\sqrt{R_1^2+R^2-2RR_1\sin(\theta_1)}+\sqrt{R_1^2+R^2+D^2-2DR_1\cos(\theta_1)-2RR_1\sin(\theta_1)}}{c} \tag{25}$$

$$\tau_{\max} = \frac{\sqrt{R_1^2+R^2+2RR_1\sin(\theta_1)}+\sqrt{R_1^2+R^2+D^2-2DR_1\cos(\theta_1)+2RR_1\sin(\theta_1)}}{c}. \tag{26}$$

page. Fig. 3 shows the AoA pdf observed at the base station.

B. AoA pdf at the Mobile Station:

Similarly, AoA pdf at MS can be obtained referring to the polar coordinate system (r_s, θ_s) at the mobile. Hence, the AoA pdf at MS is given by

$$f_{\theta_s}(\theta_s) = \frac{1}{2A}\left(r_{s2}^2(\theta_s) - r_{s1}^2(\theta_s)\right) \tag{21}$$

where

$$r_{s1}(\theta_s) = R_2\cos(\theta_s-\theta_2) - \sqrt{R_2^2\cos^2(\theta_s-\theta_2)-R_2^2+R^2} \tag{22}$$

$$r_{s2}(\theta_s) = R_2\cos(\theta_s-\theta_2) + \sqrt{R_2^2\cos^2(\theta_s-\theta_2)-R_2^2+R^2} \tag{23}$$

Substituting the value of $r_{s1}(\theta_s)$ and $r_{s2}(\theta_s)$ into (21) with $A = \pi R^2$ and simplifying results in (24) gives the AoA pdf at MS, shown at the top of the page. Fig. 4 shows the resulting AoA pdf at mobile station.

V. Marginal ToA pdf

The derivation of analytical expression for the marginal ToA pdf is in progress and will be reported in due course. ToA pdf has been evaluated through simulation and the same is in Fig. 5. The minimum and maximum value of delays given by (25) and (26), shown at the top of the page.

VI. Conclusion

Circular scattering models are used in the study of multipath characteristics of macro cellular environment. Both local and far scatterers effect the multipath characteristics of the cellular channel. In this paper we have considered only the effect of far scatterers.

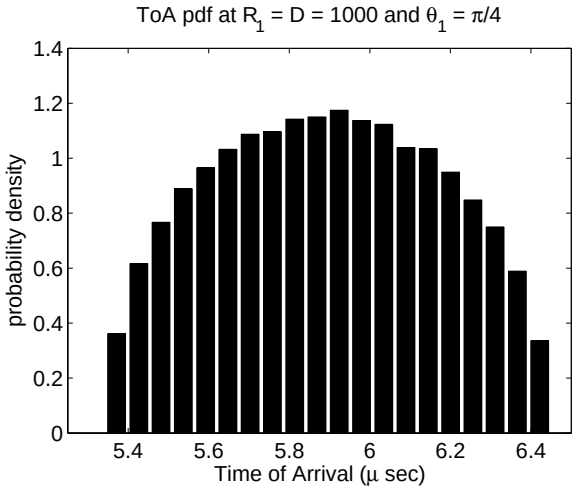

Fig. 5. ToA pdf.

For this model, analytical expressions for the joint ToA/AoA pdf and marginal AoA pdf are derived and the same has been verified through simulation. Derivation of marginal ToA pdf expression is under progress. The studies presented in this paper are expected to be useful in developing accurate geometrical based models for macro cellular environment of the cellular channel.

References

[1] R. B. Ertel, P. Cardieri, K. W. Sowerby, T. S. Rappaport, and J. H. Reed, "Overview of spatial channel models for antenna array communication systems," *IEEE Personal Commun. Mag.*, vol. 5, pp. 10–22, Feb. 1998.

[2] D. Shui, G. J. Foschini, M. J. Gans, and J. M. Kahn, "Fading correlation and its effects on the capacity of multielement antenna systems," *IEEE Trans. Commun.*, vol. 48, pp. 502–513, Mar. 2000.

[3] A. F. Molisch, "Effect of far scatterer clusters in MIMO outdoor channel models," *The 57th IEEE Semiannual Vehicular Technology Conference, 2003.*, vol. 1, pp. 534–538, Apr. 2003.

[4] H. Hofstetter, and G. Steinbock, "A geometry based stochastic channel model for MIMO systems," *ITG Workshop on Smart Antennas*, pp. 194–199, Mar. 2004.

[5] P. Almers, E. Bonek, A. Burr, N. Czink, M. Debbah, V. Degli-Esposti, H. Hofstetter, P. Kyosti, D. Laurenson, G. Matz, A. F. Molisch, C. Oestges, and H. Ozcelik, "Survey of channel and radio propagation models for wireless MIMO systems," *EURASIP Journal on Wireless Communications and Networking*, vol. 2007, pp. 1–19, Nov. 2006.

[6] P. Petrus, J. H. Reed, and T. S. Rappaport, "Geometrical-based statistical macrocell channel model for mobile environments," *IEEE Trans. on Commun.*, vol. 50, pp. 495–502, Mar. 2002.

[7] R. Janaswamy, "Angle and time of arrival statistics for the guassian scatter density model," *IEEE Trans. on Wireless Commun.*, vol. 1, pp. 488–497, Jul. 2002.

[8] R. B. Ertel, and J. H. Reed, "Angle and time of arrival statistics for circular and elliptical scattering models," *IEEE J. Select. Areas Commun.*, vol. 17, pp. 1829–1840, Nov. 1999.